Electronic Supplementary Material (ESI) for ChemComm.

Magnetic blocking in Extended Metal Atom Chains: a pentachromium(II) complex behaving as a Single-Molecule Magnet

A. Cornia,* L. Rigamonti, S. Boccedi, R. Clérac, M. Rouzières and L. Sorace

ELECTRONIC SUPPLEMENTARY INFORMATION

1. Synthesis

The H_2tpda ligand was prepared as described elsewhere, recrystallized from boiling 2-propanol and checked by ^{1}H NMR spectra and melting point measurement.[1] Naphthalene was resublimated before use. Chloroform was washed with water, stirred over $CaCl_2$ overnight and distilled under nitrogen. Diethyl ether was pre-dried over $CaCl_2$ overnight and distilled from its sodium benzophenone ketyl solution under nitrogen. *n*-Hexane was dried over 3A molecular sieves, while anhydrous dichloromethane (Aldrich) and the remaining reagents were used without further purification. All solvents were degassed by the freeze-pump-thaw technique before use. **1**$\cdot$4CHCl$_3\cdot$2Et$_2$O was synthesized in an MBraun dry box from H_2tpda, $CrCl_2$ and ^{t}BuOK in refluxing naphthalene under nitrogen (< 1 ppm H_2O and < 1 ppm O_2), following the procedure by Chang *et al.*[2] The bronze-coloured solid obtained upon complete evaporation of dichloromethane extracts was dissolved in chloroform. Diethyl ether vapours were then allowed to slowly diffuse into the filtered solution. The compound crystallized as lustrous, brown-black prisms that were easily separated from a tan powdery byproduct by flotation in Et$_2$O:CHCl$_3$ 5:1 v/v and checked by single-crystal X-Ray Diffraction (XRD), Matrix-Assisted Laser Desorption/Ionization Time-of-Flight (MALDI-ToF) and Electrospray Ionization (ESI) mass spectrometries, elemental analysis and IR spectroscopy.

Single crystal XRD (Mo-K_α, 298 K, Bruker-Nonius X8APEX four-circle diffractometer): monoclinic *C*, a = 28.51(2) Å, b = 14.04(1) Å, c = 25.08(2) Å, β = 122.90(2)°, V = 8429(11) Å^3.[2]

MALDI-ToF (CH_2Cl_2 solution, no matrix, Applied Biosystems 4800 MALDI ToF/ToF): *m*/*z* 1340.0062 ([M – Cl]$^+$, 65%), 1253.0897 ([M – CrCl$_2$]$^+$, 20%), 939.1003 (unassigned, 100%).

ESI (CH_2Cl_2 solution, direct infusion, Agilent Technologies 6310A Ion Trap LC-MS(n)): *m*/*z* 1376.2 ([M]$^+$, 100%).

Elemental analysis (crystals kept at 0.15 torr for 8 hours, Carlo Erba EA1110 CHNS-O automatic analyser). Found: C, 52.22; H, 3.29; N, 19.61. Calc. for $C_{60}H_{44}Cl_2Cr_5N_{20}$ (1376.01): C, 52.37; H, 3.22; N, 20.36%.

IR (crystals kept at 0.15 torr for 8 hours, KBr disk, FT-IR JASCO 4700, resolution 2 cm^{-1}): ν_{max}/cm^{-1} 1604, 1578, 1548, 1474, 1453, 1422, 1408, 1348, 1335, 1155.[2]

2. Direct-current (dc) and alternating-current (ac) magnetic measurements

The magnetization and magnetic susceptibility measurements were carried out with the use of MPMS-XL Quantum Design SQUID magnetometer and PPMS-9 susceptometer. The MPMS-XL instrument works between 1.8 and 400 K with applied dc fields ranging from -7 to 7 T. Ac susceptibility measurements were made with an oscillating field of 5 Oe with frequency from 1 to 1500 Hz (MPMS) and with an oscillating field of 1 Oe with frequency from 10 to 10000 Hz (PPMS). The magnetic data were corrected for the sample holder, paratone oil and the intrinsic diamagnetic contributions estimated through Pascal's constants. Measurements were performed on two polycrystalline samples:

(*a*) **1**$\cdot 4CHCl_3 \cdot 2Et_2O$ covered and thus restrained in a minimum amount of frozen mother liquor (17.23 mg) within a sealed straw to prevent desolvation of the solid. No evaporation of the mother liquor was observed during the measurements. The mass of the sample was estimated at about 13.2 mg after the measurements and right after the mother liquor removal/evaporation (about 5 minutes) under argon. It is worth noting that under the microscope the crystals were looking perfectly shiny and crystalline immediately after removal of the mother liquor. Nevertheless, because residues of solvent could easily alterate the mass of the sample, the actual mass was accurately determined (11.35 mg) by comparing the high-temperature magnetic data with those of the dry compound (see below).

(*b*) **1** (6.44 mg) obtained by keeping crystals of **1**$\cdot 4CHCl_3 \cdot 2Et_2O$ under vacuum on a Schlenk line for 5 hours; thus the used molar mass (1375.96 g/mol) did not include the interstitial solvent molecules. The sample was covered with paratone oil to avoid magnetic torqueing and introduced in a sealed polyethylene bag (3 × 0.5 × 0.02 cm).

Prior to the experiments, the field-dependent magnetization was measured at 100 K on each sample in order to detect the presence of any bulk ferromagnetic impurities. In fact, paramagnetic or diamagnetic materials should exhibit a perfectly linear dependence of the magnetization that extrapolates to zero at zero dc field. The samples appeared to be free of any significant ferromagnetic impurities. The susceptibility (normalized per $[Cr_5]$ unit) so obtained from the slope of the *M versus H* plots at 100 K was 0.0288 cm^3 mol^{-1} for both samples, in good agreement with the susceptibility measurements at 1 and 10 kOe (see below). The dc magnetic susceptibility was obtained as *M*/*H* from magnetization measurements at 1 and 10 kOe in the temperature range 1.86-

255 K for **1**·4CHCl$_3$·2Et$_2$O and 1.85-320 K for **1**. Magnetization data were recorded at eight temperatures from to 1.9 to 10 K (1.9, 2.0, 3.0, 4.0, 5.0, 6.0, 8.0, 10.0 K) in fields up to 70 kOe for both samples. Above 1.8 K, no hysteresis effects (at about 70 to 600 Oe/min) were observed on the field dependence of the magnetization. Ac susceptibility data were taken up to 1500 Hz and 10000 Hz for **1**·4CHCl$_3$·2Et$_2$O (1.86–15.0 K) and **1** (1.8–15.0 K), respectively. For both samples it was not possible to observe slow relaxation of the magnetization in zero dc field in the available temperature and frequency ranges. All ac measurements were fitted to the generalized Debye model (using χ' and χ'' *versus* ν data)[3] in order to extract the characteristic relaxation frequency, the α parameter describing the width of the distribution of relaxation times, as well as the values of χ_0-χ_∞, χ_0 and χ_∞. The α values decreased from ~0.2 at the lowest temperatures to ~0 upon heating.

Spin-Hamiltonian calculations were carried out using in-house developed software based on ZHEEV routine[4] for matrix diagonalization and E04FCF routine[5] for least-square fitting over magnetization values. For **1**·4CHCl$_3$·2Et$_2$O, 912 datapoints at 1.9, 2.0, 3.0, 4.0, 5.0, 6.0, 8.0 and 10.0 K were fitted to the zero-field splitting *plus* Zeeman hamiltonian in Eq. (S1) using isotropic g, D and a preferential orientation coefficient a_2 as adjustable parameters.

$$\hat{\mathbf{H}}_{\mathrm{zfs+Zee}} = D[\hat{S}_{\mathrm{T},z}{}^2 - S_\mathrm{T}(S_\mathrm{T}+1)/3] + g\mu_\mathrm{B}\hat{\mathbf{S}}_\mathrm{T}\cdot\hat{\mathbf{H}} \qquad \text{(S1)}$$

When preferential orientation effects were not included, the sum-of-squares was ~280 times larger and an accurate fitting was impossible. A similar situation was already encountered in the past in our lab: it was shown to arise from a nonstatistical distribution of crystal orientations in samples comprising a small number of large crystals, and not from field-induced torqueing. Preferential orientation effects were modeled with an axial probability function[6] expressed as a linear combination of Legendre polynomials of even order, including only $P_0(\cos\theta) = 1$ and $P_2(\cos\theta) = \frac{1}{2}(3\cos^2\theta - 1)$. The value of a_0 is fixed by the normalization condition, while the negative value of a_2 (Figures S2 and S3) indicates an oblate distribution of the easy axes, *i.e.* the "parallel" arrangement is less populated than in a randomly-oriented sample. For **1**, 904 datapoints at 1.9, 2.0, 3.0, 4.0, 5.0, 6.0, 8.0 and 10.0 K were fitted using only isotropic g and D as adjustable parameters in Eq. (S1).

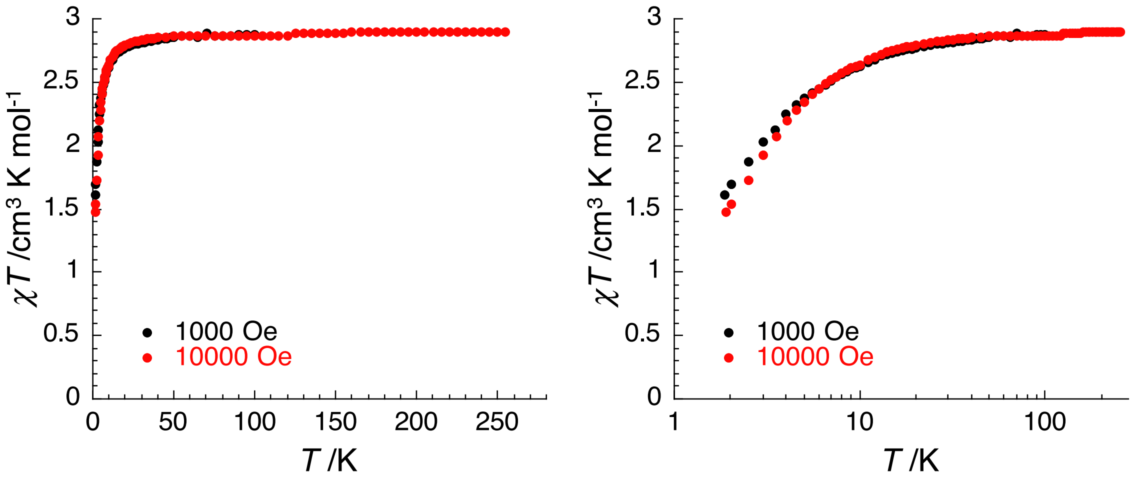

Figure S1. χT *versus* T plot for **1**·4CHCl$_3$·2Et$_2$O in the temperature range 1.86–255 K at two different values of the applied field (1 and 10 kOe). At the highest temperatures reached, the χT product is 2.89 cm^3 K mol^{-1}. When the temperature is lowered, the χT product at 1 kOe decreases reaching 1.61 cm^3 K mol^{-1} at 1.86 K.

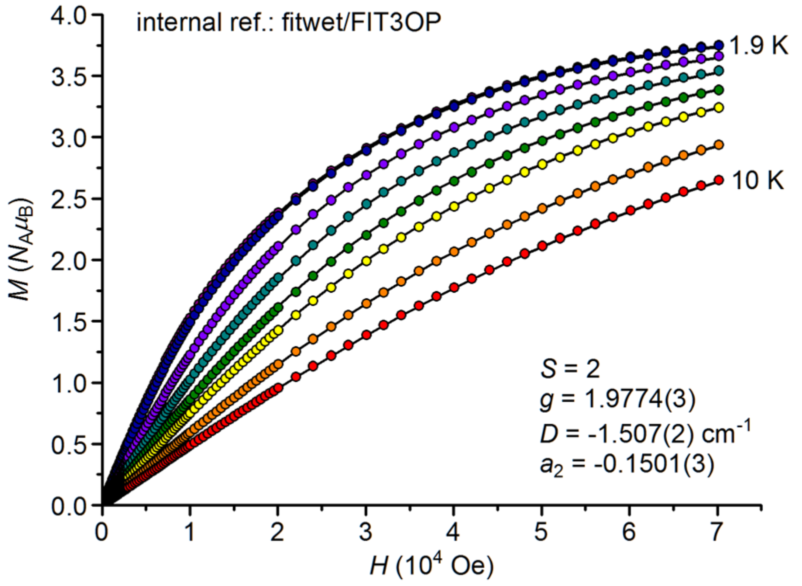

Figure S2. M *versus* H plot for **1**·4CHCl$_3$·2Et$_2$O at eight temperature values between 1.9 and 10 K (1.9, 2.0, 3.0, 4.0, 5.0, 6.0, 8.0, 10.0 K). The solid curves provide the best fit to experimental data with the reported set of parameters. The highest magnetization value detected is 3.75 $N_A\mu_B$ at 1.9 K and 70 kOe.

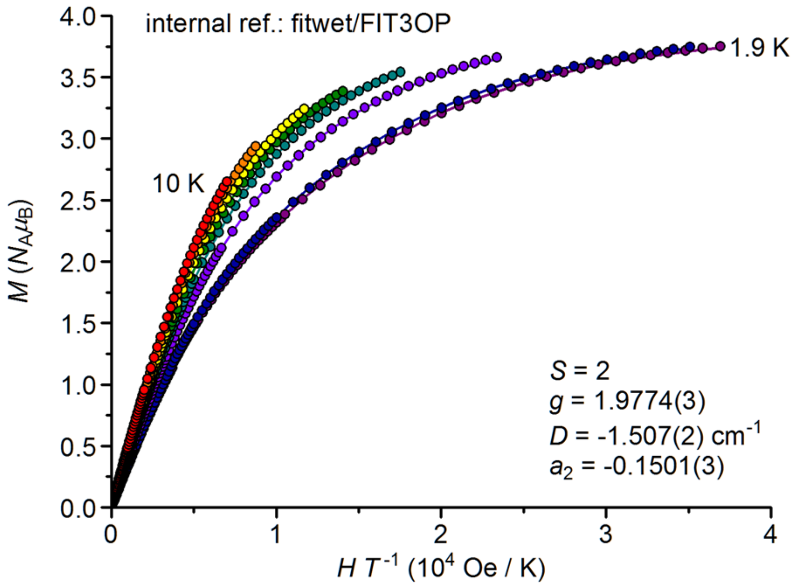

Figure S3. *M versus H/T* plot for **1**$\cdot 4CHCl_3 \cdot 2Et_2O$ at temperatures between 1.9 and 10 K (1.9, 2.0, 3.0, 4.0, 5.0, 6.0, 8.0, 10.0 K). The solid curves provide the best fit to experimental data with the reported set of parameters.

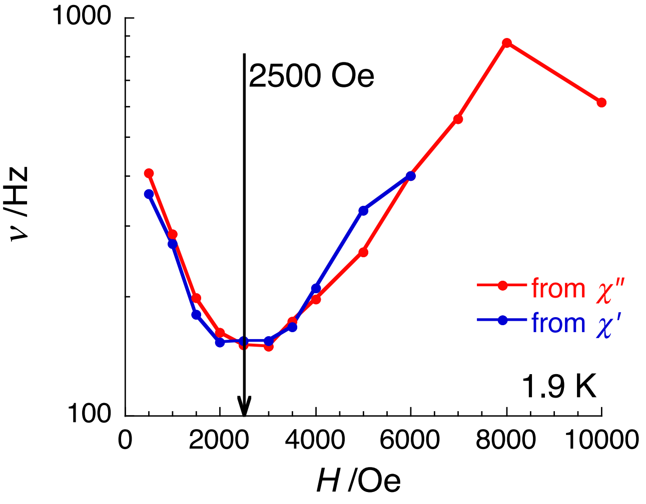

Figure S4. Characteristic relaxation frequency of **1**$\cdot 4CHCl_3 \cdot 2Et_2O$ as a function of applied static field at 1.9 K. The slowest relaxation occurs at 2.5 kOe.

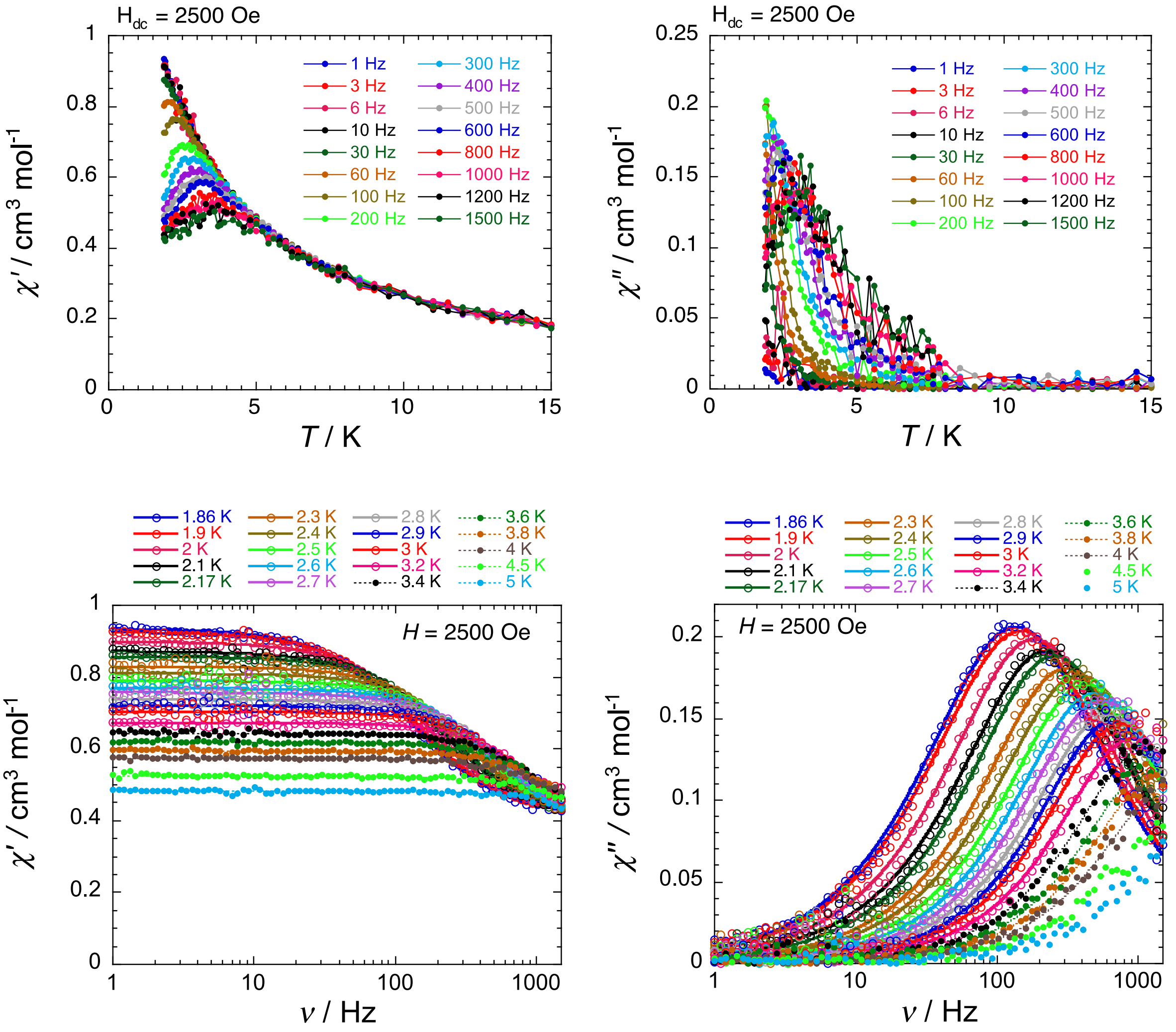

Figure S5. In-phase (left) and out-of-phase (right) components of the molar ac magnetic susceptibility of **1**·$4CHCl_3 \cdot 2Et_2O$ measured as a function of temperature at different frequencies (top) and as a function of frequency at different temperatures (bottom) at 2.5 kOe. While solid lines on the top figures are visual guides, the solid curves on the bottom figures provide the best fit using the generalized Debye model.[3]

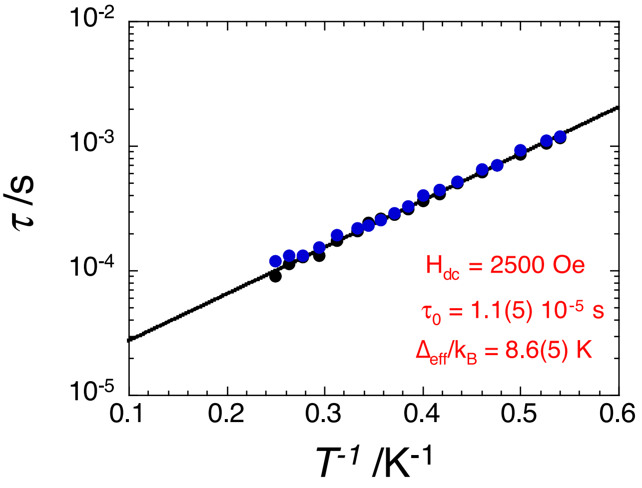

Figure S6. Temperature dependence of the relaxation time of **1**·$4CHCl_3 \cdot 2Et_2O$ at 2.5 kOe extracted from χ' *versus* ν (blue dots) and χ'' *versus* ν (black dots) curves between 1.86 and 4 K. The solid line provides the best fit to Arrhenius law with the reported parameter set.

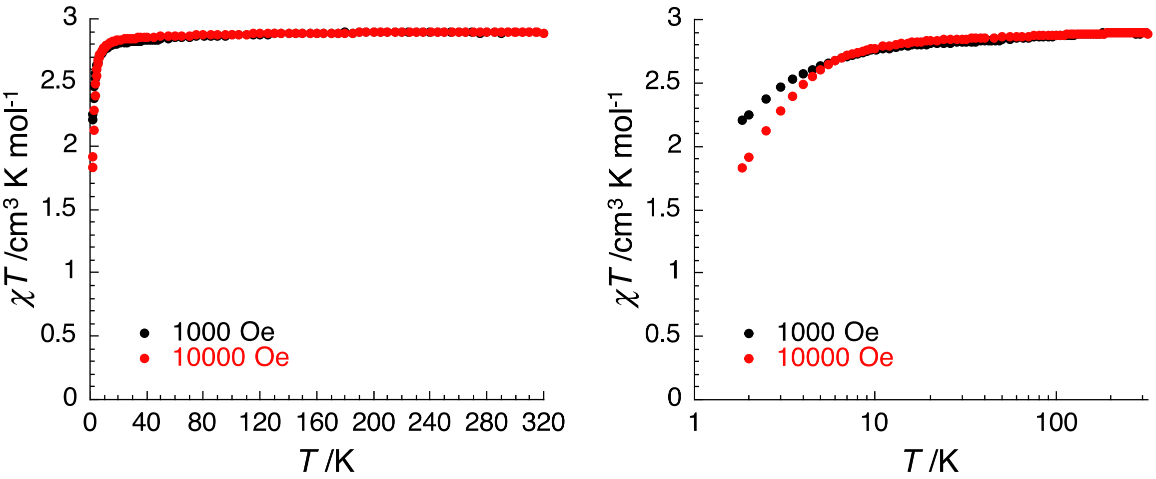

Figure S7. χT *versus* T plot for **1** in the temperature range 1.85-320 K at two different values of the applied field (1 and 10 kOe). At room temperature, the χT product is 2.89 cm^3 K mol^{-1}. When the temperature is lowered, the χT product at 1 kOe decreases reaching 2.21 cm^3 K mol^{-1} at 1.85 K.

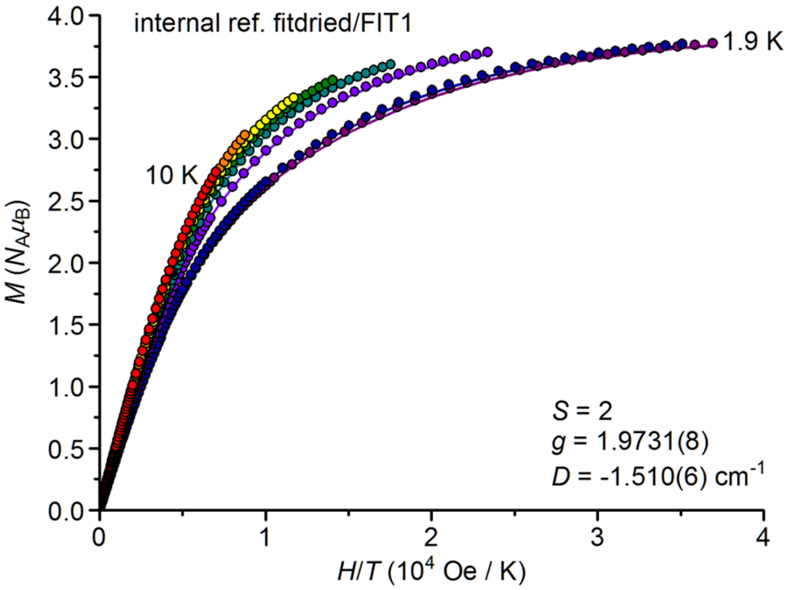

Figure S8. *M versus H/T* plot for **1** at temperatures between 1.9 and 10 K. The solid curves provide the best fit to experimental data with the reported set of parameters.

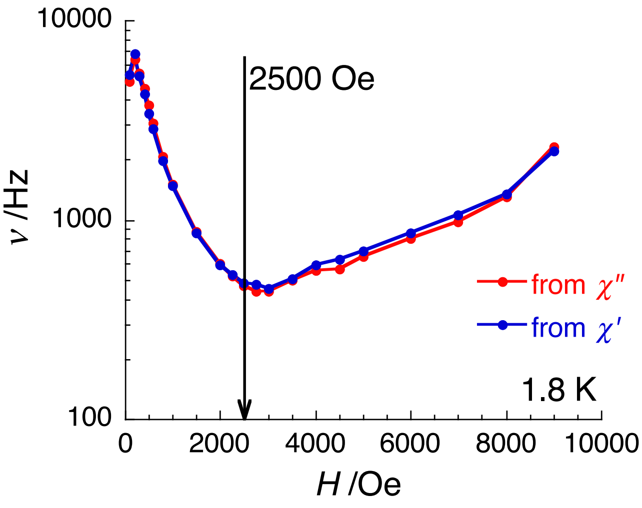

Figure S9. Characteristic relaxation frequency of **1** as a function of applied static field at 1.8 K. The slowest relaxation occurs at 2.5 kOe.

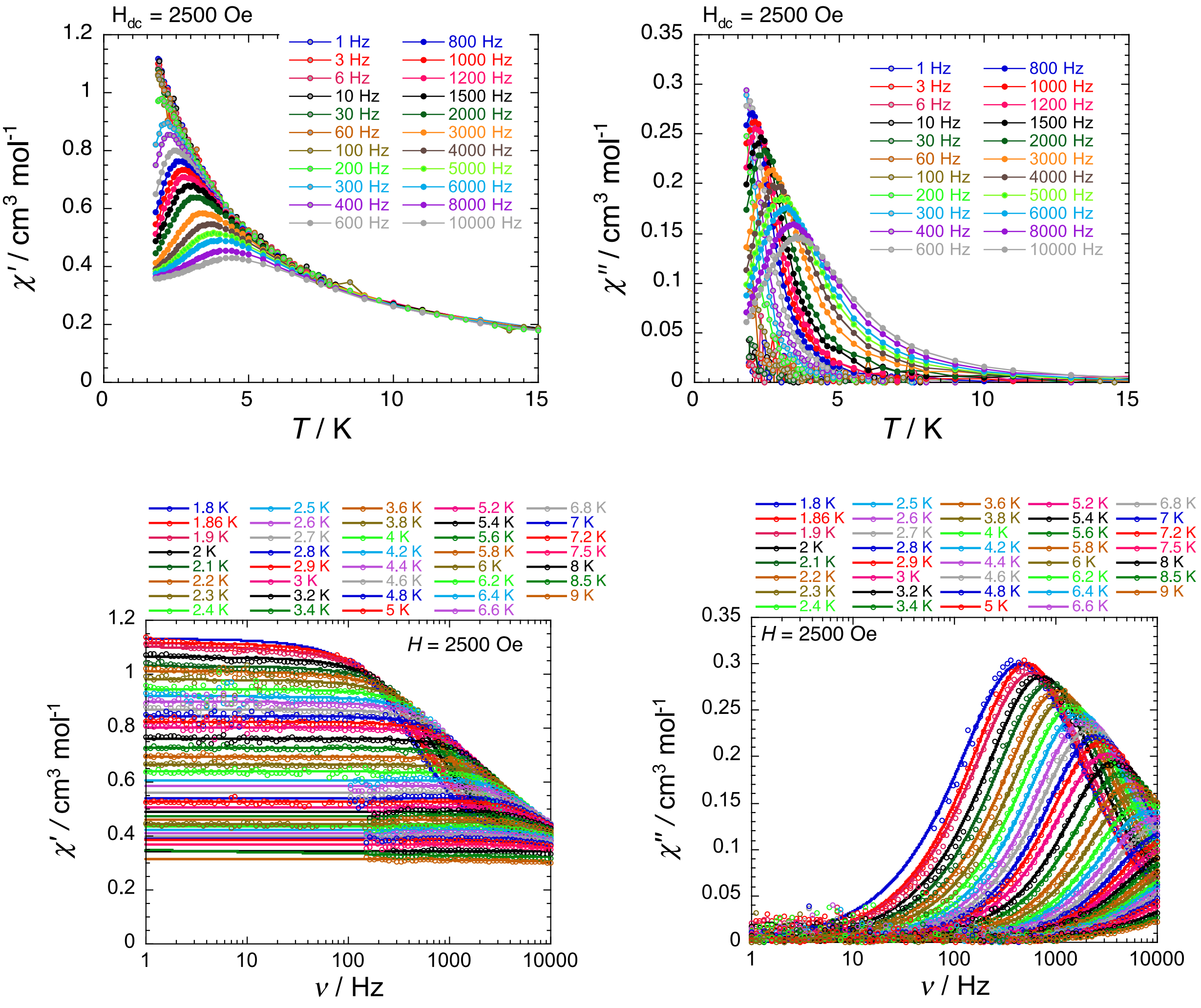

Figure S10. In-phase (left) and out-of-phase (right) components of the molar ac magnetic susceptibility of **1** measured as a function of temperature at different frequencies (top) and as a function of frequency at different temperatures (bottom) at 2.5 kOe. While solid lines on the top figures are visual guides, the solid curves on the bottom figures provide the best fit using the generalized Debye model.[3]

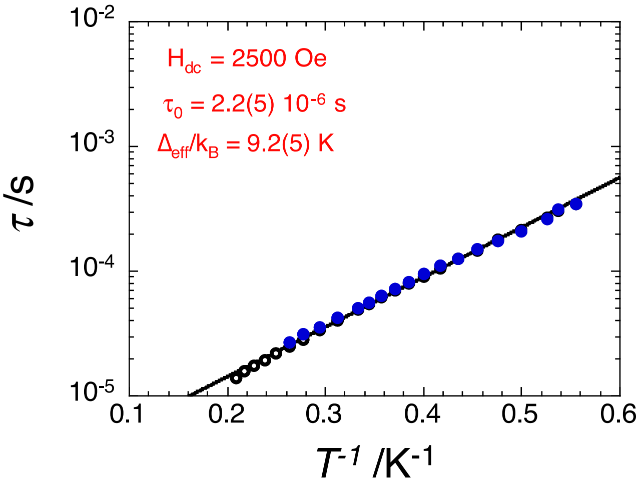

Figure S11. Temperature dependence of the relaxation time of **1** at 2.5 kOe extracted from χ' *versus* ν (blue dots) and χ'' *versus* ν (black dots) curves between 1.8 and 4.8 K. The solid line provides the best fit to Arrhenius law with the reported parameter set.

3. EPR measurements

W-band EPR spectra were recorded on a Bruker Elexsys E600 spectrometer, equipped with a CF935 ^{4}He cryostat (Oxford Instruments) to work at low temperature. Sample was obtained by roughly grinding a large crystal covered with paratone in a glove-box. This was then mixed with wax inserted in an open end W-band EPR tube (0.8 mm external diameter). To further reduce exposition of the sample to air, the tube was taken out from the glove-box in a sealed Schlenk, mounted on the sample holder rod under nitrogen flux, pre-cooled in a bath of liquid N_2 and inserted in the spectrometer at 100 K.

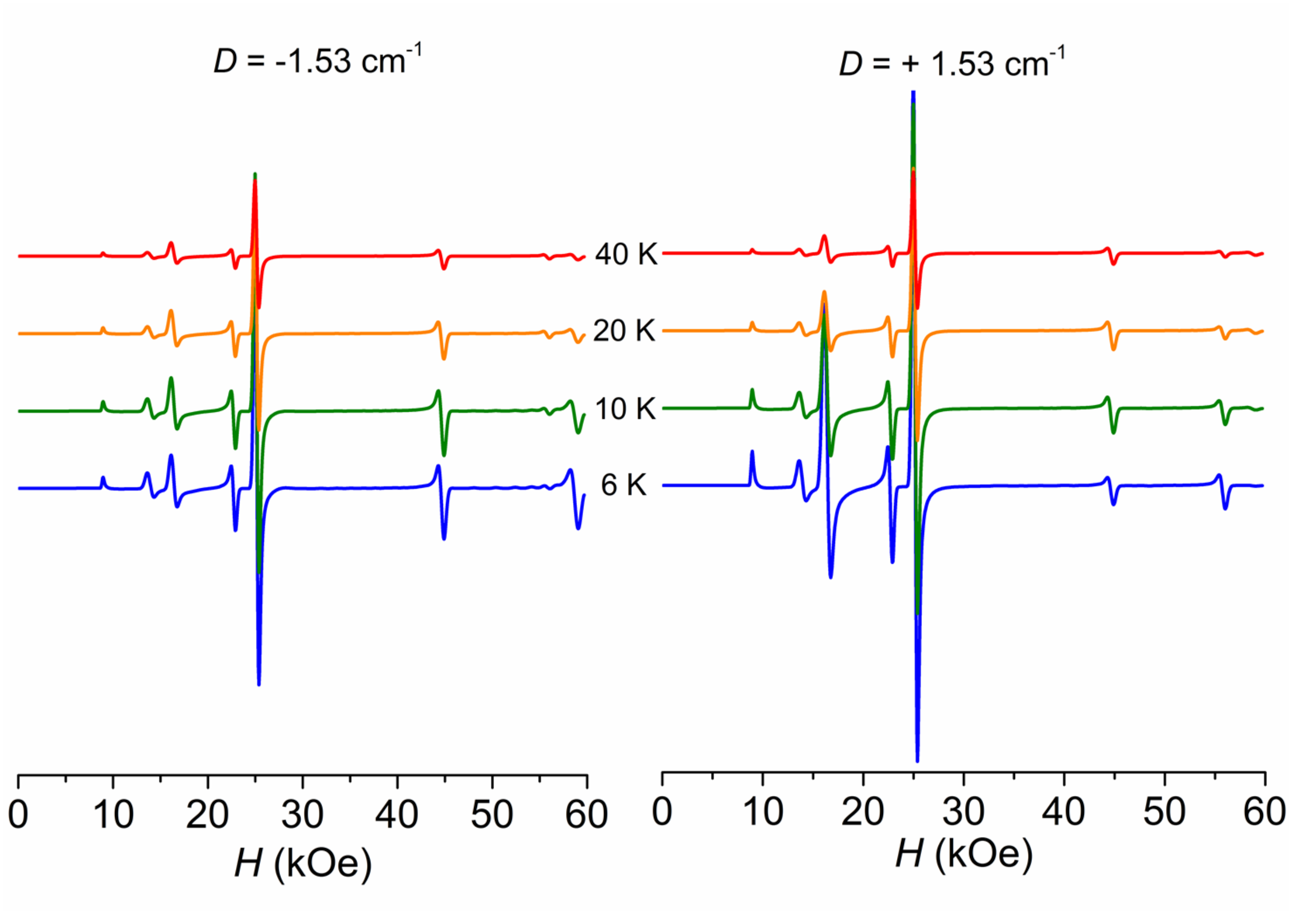

Figure S12 Comparison of the temperature-dependent simulated EPR spectra for **1** obtained by using $g_x = g_y = 1.99$, $g_z = 1.975$, $E = 0.006$ cm^{-1} and $D < 0$ (left) or $D > 0$ (right).

4. Angular Overlap Model (AOM) calculations

The calculations were performed using a previously described program,[7] starting from the angular coordinates of the four nitrogens and of the chlorine atom obtained from the crystal structure. The ligand field was modeled by using standard B, C, ζ, k parameters and ligand field parameters capable of providing a reasonable reproduction of the electronic spectra reported in literature for [Cr(Mepy)$_4$Cl$_2$] (see Table S1).[8] This was obtained by considering a completely anisotropic π-interaction for the pyridine-type ligands, and a completely isotropic π–interaction for the chloride ligand. The effect of the neighbouring {Cr$_2$} unit was then taken into account by substituting one of the chlorides of [Cr(Mepy)$_4$Cl$_2$] either with no ligand, with a simple σ–acceptor, or with a $\sigma + \pi$ acceptor.[9] At any rate, the calculated zero-field splitting parameters were only weakly affected by the way {Cr$_2$} ligand field was modelled, and in good agreement with those experimentally determined.

Table S1. Ligand field parameters used for the AOM calculations of the electronic structure of Cr1 in **1** and spin-Hamiltonian (SH) parameters that result from varying the effect of the neighboring {Cr_2} unit.

Ligand field parameters	Value	Calculated SH parameters	$10Dq(Cr_2) = 0$	$10Dq(Cr_2)$=-5000 cm^{-1} $e_\pi/e_\sigma = 0$	$10Dq(Cr_2)$ =-5000 cm^{-1} e_π/e_σ=0.3
B / cm^{-1}	800	D/ cm^{-1}	-1.47	-1.36	-1.38
C / cm^{-1}	3300	E/ cm^{-1}	3.8 x 10^{-3}	2.7 x 10^{-3}	2.6 x 10^{-3}
ζ / cm^{-1}	235	g_x	1.998	1.998	1.998
K	0.82	g_y	1.998	1.998	1.998
$10Dq$(N)/ cm^{-1}	16500	g_z	1.978	1.977	1.978
$10Dq$(Cl)/ cm^{-1}	5000				
e_π/e_σ	0.30				
$e_{\pi c}$(N)/ $e_{\pi s}$(N)	0.0				
$e_{\pi c}$(Cl)/ $e_{\pi s}$(Cl)	1.0				

5. References

1. (*a*) S.-J. Shieh, C.-C. Chou, G.-H. Lee, C.-C. Wang and S.-M. Peng, *Angew. Chem. Int. Ed.*, 1997, **36**, 56–59; (*b*) C. C. Wang, W.-C. Lo, C.-C. Chou, G.-H. Lee, J.-M. Chen and S.-M. Peng, *Inorg. Chem.*, 1998, **37***,* 4059–4065.
2. H.-C. Chang, J.-T. Li, C.-C. Wang, T.-W. Lin, H.-C. Lee, G.-H. Lee and S.-M. Peng, *Eur. J. Inorg. Chem.*, 1999, 1243–1251.
3. (*a*) K. S. Cole and R. H. Cole, *J. Chem. Phys.*, 1941, **9**, 341–352; (*b*) C. Dekker, A. F. M. Arts, H. W. Wijn, A. J. Duyneveldt and J. A. Mydosh, *Phys. Rev. B*, 1989, **40**, 11243–11251.
4. ZHEEV LAPACK Driver Routine (version 2.0), Univ. of Tennessee, Univ. of California Berkeley, NAG Ltd., Courant Institute, Argonne National Lab, and Rice University, USA, 1994.
5. E04FCF, NAG Fortran Library Routine (Mark 17), NAG Ltd, Oxford, UK, 1996.
6. N. A. Chumakova, T. S. Yankova and A. Kh. Vorobiev, *Appl. Magn. Reson.*, 2008, **33**, 117–126.
7. A. Bencini, I. Ciofini, M. Uytterhoeven, *Inorg. Chim. Acta*, 1998, **274**, 90–101.
8. A. B. P. Lever, *Inorganic Electronic Spectroscopy*, Elsevier, Amsterdam, The Netherlands, 2nd edn., 1986.
9. K.-W. Lee and P. E. Hoggard, *Inorg. Chem.*, 1990, **29***,* 850–854.